Spherical-wave computational AVO modelling in elastic and anelastic isotropic two-layer media

Arnim B. Haase and Charles P. Ursenbach
CREWES, University of Calgary

Summary

Compressional-wave AVO responses and converted-wave AVO responses in elastic and anelastic two-layer isotropic Class 1 models are investigated. These responses are computed by utilizing Zoeppritz reflection coefficients and the Weyl/Sommerfeld-integral. Spherical-wave depth dependence for PP and PSv Class 1 models is found to be strongest near the critical angle. The constant-Q approximation is used to introduce anelastic effects. AVO responses of two-layer isotropic models are sensitive to anelasticity. However, when unit reflectivity scaling is employed to compensate for attenuation of reflection amplitudes, computed AVO characteristics are comparable to the elastic situation. For Class 1 spherical-wave AVO the Q-factor dependence is strongest near critical angles. This Q-dependence is similar to the depth dependence of elastic comparisons.

Introduction

Amplitude-versus-offset (AVO) analysis was introduced by Ostrander (1984). It is also discussed in a paper by Hron et al. (1986) as amplitude versus distance. AVO analysis and AVO inversion are now widely accepted tools in seismic exploration. Linear approximations of the Zoeppritz equations are commonly used to implement plane wave analysis. Small incidence angles and small parameter changes are assumed for these approximations. At larger angles linearized approximations begin to break down and they are not applicable near critical points. Even "exact Zoeppritz" is a plane wave approximation to the real world. What, then, is the spherical-wave response for AVO Class 1? Krail and Brysk (1983) attempted to address this question, but incorporated a number of approximations, not all of which are valid at critical angles. The only approximation in the modelling study presented here is the assumption that compressional wave particle motion is parallel to the propagation direction and that converted-wave particle motion is perpendicular to the propagation direction.

Anelasticity of some degree is found in all rocks encountered in nature. Anelasticity causes attenuation and velocity dispersion of seismic waves. Velocity dispersion means velocities are functions of frequency. This frequency dependence of seismic velocities can be quantified by the frequency-independent quality factor Q (Kjartansson, 1979). It is well known that plane wave AVO responses are Q-factor dependent (see for example Carcione et al., 1998). Naturally, spherical-wave AVO responses are also expected to be Q-factor dependent. This modelling study also seeks to quantify the sensitivity of Class 1 spherical-wave AVO responses with respect to finite Q-factors.

Potentials and displacements

Plane-wave particle motion reflection and transmission coefficients for elastic isotropic media in welded contact are given by the Zoeppritz equations. The formalism for expressing spherical wave fronts as contour integrals over plane waves goes back to Weyl (1919). Aki and Richards (1980, p217) derive equations for generalized PP-reflections and generalized PSv-reflections in terms of potentials Φ (Equation 1) and Ψ (Equation 2):

$$\Phi = Ai\omega e^{-i\omega t}\int_0^\infty R_{\mathrm{PP}}(p)\frac{p}{\xi}J_0(\omega pr)e^{i\omega\xi(z+h)}dp \quad , \tag{1}$$

$$\Psi = Ai\omega e^{-i\omega t}\int_0^\infty \left(\frac{1}{i\omega p}\frac{\beta}{\alpha}R_{\mathrm{PS}}(p)\right)\frac{p}{\xi}J_0(\omega pr)e^{i\omega(\xi h+\eta z)}dp \quad . \tag{2}$$

[Notation is similar to Aki and Richards (1980).] Reflections from an elastic interface are computed firstly by introducing particle motion reflection coefficients given by the Zoeppritz equations. Secondly, particle motion **u** is computed from Equation (3)

$$u = \nabla\Phi + \nabla\times\nabla\times(0,0,\Psi) \quad , \tag{3}$$

and from the potentials given by Equations (1) and (2). Next it is assumed that displacement is parallel to the ray direction for PP reflected waves, and perpendicular for converted waves. Other displacement components are neglected. [This is the sole approximation in the procedure and introduces very little error (Ursenbach et al., 2005).] The p-integrations proceed for a single frequency point. They are repeated for all frequency points desired in the output bandwidth, and then the time domain response is found by inverse Fourier transform. Quadrature traces are determined by Hilbert transform, and the maximum instantaneous amplitude yields the peak response at the receiver. When corrected for spherical spreading, this gives an estimate of the reflection coefficient.

Attenuation and dispersion

A mathematical treatment of anelasticity can be found in Aki and Richards (1980). They show that causality requires velocity dispersion, for which they derive the following approximate expression:

$$v(\omega) = v_{ref}\left(1+\ln\left(\omega/\omega_{ref}\right)/(\pi Q)-\frac{i}{2Q}\right) \qquad (4)$$

where Q is a frequency-independent quality factor. The values v_{ref} and ω_{ref} are assumed known. As in the elastic case before, spherical-wave displacements **u** are computed from the potentials Φ and Ψ. The integrations shown in Equations 1 and 2 again proceed one frequency point at a time. However, in the anelastic situation velocities are complex and must be recomputed for every frequency point, according to Equation 4. The P-wave quality factor for the top layer (Q_{P1}) is assumed to be known for the computations and is listed in the figures. Q_{P2} (for the bottom layer) as well as S-wave quality factors Q_{S1} and Q_{S2} are calculated with the aid of empirical equations (Waters, 1978; Udias, 1999):

$$1/Q_P = \left(\frac{const.}{\alpha}\right)^2, \qquad (5) \qquad\qquad Q_S = Q_P\,\frac{4}{3}\left(\frac{\beta}{\alpha}\right)^2. \qquad (6)$$

Modelling results

An actual gas-sand reservoir from western Canada is utilized to derive two-layer models for this study. Density ρ_1 is 2400 kg/m^3 for the layer just above the reservoir. P-wave velocity α_1 = 2000 m/s is dictated by a reservoir depth of 500 m and a corresponding two-way travel time of approximately 500 ms. The layer parameters for AVO Class 1 shown in Table 1 are adapted from Rutherford and Williams (1989). Output signal bandwidth and linear edge tapers are determined by choosing a 5/15-80/100 Hz Ormsby wavelet as the source signature. Free surface effects are not considered in this study. A P-wave point source and spherical incident wave fronts are assumed for the computations. The appearance of computed AVO results depends on scaling. Spherical spreading must be compensated for if results are to be compared to plane-wave responses. All normalization factors used to compute Figures 1 and 3 are derived by setting reflection coefficients R in Equations 1 and 2 to unity. The *trace* displays (Figures 2 and 4) are scaled individually in order to accommodate maximum amplitudes. Clipping of maximum trace amplitudes is indicated by colour changes. Figure 1 shows elastic AVO response magnitudes computed from trace envelopes. AVO Class 1 comparisons are given in Figure 1a for pressure waves and in Figure 1b for converted waves. Plane-wave comparisons are added to all AVO magnitude responses in order to highlight the impact of spherical wave fronts. Figure 2 displays the corresponding spherical-wave *traces*, from which, after normalization, Figure 1 may be derived.

The same two layer model as was utilized in the elastic situation is also employed in the anelastic study. All velocities listed in Table 1 are taken to be reference velocities here; the reference frequency (see Equation 4) is set to 50 Hz. As before, a 5/15-80/100 Ormsby wavelet is chosen as the source signature; a P-wave point source is assumed. Free surface effects are ignored. Calculations are performed for two different values of the top layer P-wave quality-factor: firstly, Q_{P1} = 100 and, secondly, Q_{P1} = 387.5 . The other Q-factors are calculated from Equations 5 and 6 and are listed in Table 2. Figures 3 and 4 display the anelastic analogues to Figures 1 and 2. Figure 3 shows anelastic Class 1 spherical-wave AVO responses. Plane-wave and elastic spherical-wave responses are given for comparison. PP- and PSv-reflection *traces* for AVO Class 1 of the anelastic case are displayed in Figure 4.

Table 1 Layer parameters.

α_1/[m/s]	β_1/[m/s]	ρ_1/[kg/m^3]	α_2/[m/s]	β_2/[m/s]	ρ_2/[kg/m^3]
2000	879.88	2400	2933.33	1882.29	2000

Table 2 Derived Q-factors.

Q_{p1}	Q_{p2}	Q_{s1}	Q_{s2}
100	215.1	25.8	118.1
387.5	833.5	100	457.6

Discussion and conclusions

For Class 1 AVO models, the P-wave velocity is increasing across the interface as can be seen in Table 1. Because of this velocity increase a critical angle exists and head waves are generated in Class 1 models. A head wave can be seen separating from reflected waves at the highest angles in Figure 2b. The PSv-reflection *traces* in Figure 2b start with zero amplitude at zero angle. Next, a negative reflection amplitude grows stronger towards a magnitude maximum just below 30˚. Beyond 30˚ the PSv-reflection strength diminishes first and then goes through a phase rotation and increases in strength near the critical angle (just beyond 40˚). With angles increasing beyond that, the reflection amplitude becomes negative again and diminishes towards zero at 90˚. Figure 1a shows the magnitude of R_{PP} for Class 1. The greatest departure from a plane-wave comparison is observed in the vicinity of the critical angle. Normalized *Q*-dependence for spherical-wave AVO Class 1, as shown in Figure 3, to some degree mimics normalized depth dependence of the elastic situation (see Figure 1). Increasing *Q*-factors and increasing depths move normalized spherical-wave AVO closer to plane-wave comparisons. The *trace* plots in Figure 4 show phase rotations when compared to the elastic situation (Figure 2). Note that these *trace* examples are all computed for a depth level of 500 m and $Q = 100$ for attenuation. Amplitude clipping is indicated by colour changes. Also noticeable in these trace plots is the increased pulse width of anelastic converted wave reflections. This wavelet stretch is indicative of a spectral band narrowed by predominant attenuation of higher frequencies.

In summary, exact spherical-wave reflection coefficients may be calculated numerically by integration over the plane-wave coefficients, R_{PP} and R_{PS}. Scaling by similar results obtained using unit reflectivity allows one to identify fundamental deviations from plane-wave behaviour. Class 1 models show significant amplitude deviations and phase rotations near the critical angle. This is observed even for depths of 2000 m. Class 1 spherical PSv-wave AVO is more sensitive to decreasing *Q*-factors than its Class 1 PP-wave comparison.

Acknowledgements

The authors wish to thank Professor E. Krebes for helpful discussions related to the theory. Support from CREWES and its industrial sponsorship is gratefully acknowledged.

References

Aki, K.T., and Richards, P.G. [1980] *Quantitative Seismology: Theory and Methods. Vol. 1*, W.H. Freeman and Co.

Carcione, J.M., Helle, H.B., and Zhao, T. [1998] Effects of attenuation and anisotropy on reflection amplitude versus offset. *Geophysics*, **63**, 5, 1652-1658.

Hron, F., May, B.T., Covey, J.D., and Daley, P.F. [1986] Synthetic seismic sections for acoustic, elastic, anisotropic, and vertically inhomogeneous layered media. *Geophysics*, **51**, 3, 710-735.

Kjartansson, E. [1979] Constant Q, wave propagation and attenuation. *Journal of Geophysical Research*, **84**, 4737-4748.

Krail, P.M., and Brysk, H. [1983] Reflection of spherical seismic waves in elastic layered media. *Geophysics*, **48,** 6, 655-664.

Ostrander, W.J. [1984] Plane-wave reflection coefficients for gas sands at nonnormal angles-of –incidence. *Geophysics*, **49,** 10, 1637-1648.

Rutherford, S.R., and Williams, R.H. [1989] Amplitude-versus-offset variations in gas sands. *Geophysics*, **54**, 6, 680-688.

Udias, A. [1999] *Principles of seismology*. Cambridge University Press, page 260.

Ursenbach, C.P., Haase, A.B., and Downton, J.E. [2005] An efficient method for AVO modeling of reflected spherical waves. 75th SEG meeting, Expanded Abstracts, 202-205.

Waters, K.H. [1978] *Reflection Seismology*. John Wiley and Sons, Inc., page 203.

Weyl, H. [1919] Ausbreitung elektromagnetischer Wellen ueber einem ebenen Leiter. *Ann. Physik*, **60**, 481-500.

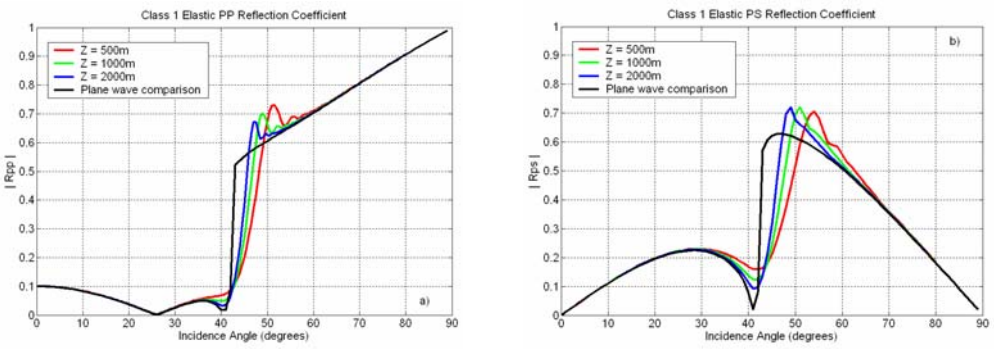

Figure 1 Spherical-wave reflection coefficients for Class 1 AVO, (a) PP (b) PSv

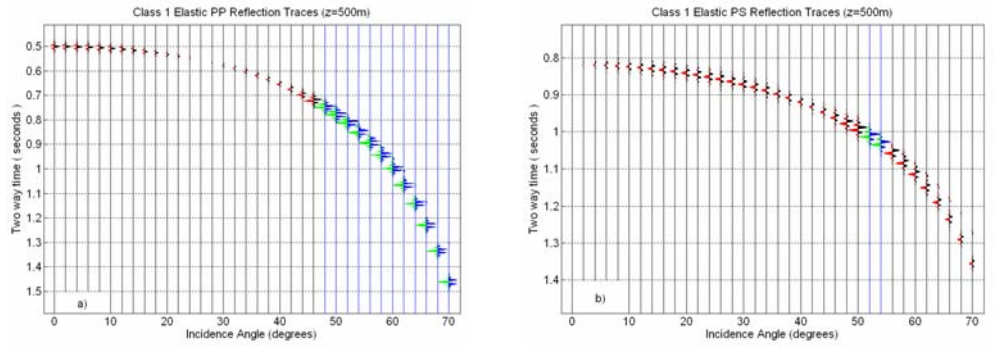

Figure 2 Spherical-wave reflection traces for Class 1 AVO, (a) PP (b) PSv

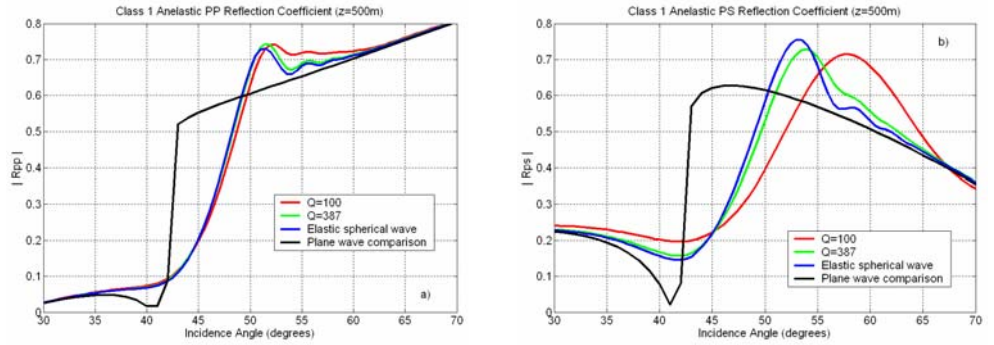

Figure 3 Anelastic spherical-wave reflection coefficients for Class 1 AVO, (a) PP (b) PSv

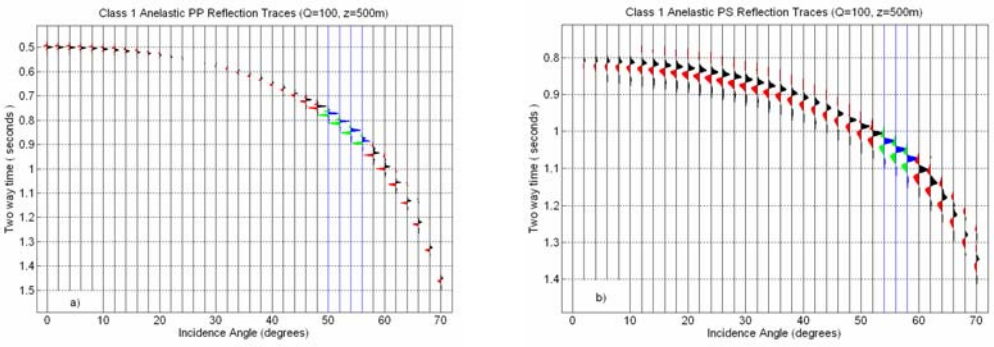

Figure 4 Anelastic spherical-wave reflection traces for Class 1 AVO, (a) PP (b) PSv